Additive Manufacturing Frontiers 4 (2025) 200196

Contents lists available at ScienceDirect

Additive Manufacturing Frontiers

journal homepage: www.elsevier.com/locate/amf

Machine Learning-Based Online Monitoring and Closed-Loop Controlling for 3D Printing of Continuous Fiber-Reinforced Composites

Xinyun Chi [a,1], Jiacheng Xue [a,1], Lei Jia [b], Jiaqi Yao [a], Huihui Miao [a], Lingling Wu [a,*], Tengfei Liu [a], Xiaoyong Tian [a,*], Dichen Li [a]

[a] State Key Laboratory for Manufacturing Systems Engineering, Xi'an Jiaotong University, Xi'an, 710049, China
[b] China Academy of Launch Vehicle Technology, Beijing, 100076, China

A R T I C L E I N F O

Keywords:
Continuous fiber-reinforced composites
3D printing
Computer vision
Machine learning
Defect detection
Feedback control

A B S T R A C T

Ensuring the consistent mechanical performance of three-dimensional (3D)-printed continuous fiber-reinforced composites is a significant challenge in additive manufacturing. The current reliance on manual monitoring exacerbates this challenge by rendering the process vulnerable to environmental changes and unexpected factors, resulting in defects and inconsistent product quality, particularly in unmanned long-term operations or printing in extreme environments. To address these issues, we developed a process monitoring and closed-loop feedback control strategy for the 3D printing process. Real-time printing image data were captured and analyzed using a well-trained neural network model, and a real-time control module-enabled closed-loop feedback control of the flow rate was developed. The neural network model, which was based on image processing and artificial intelligence, enabled the recognition of flow rate values with an accuracy of 94.70 %. The experimental results showed significant improvements in both the surface performance and mechanical properties of printed composites, with three to six times improvement in tensile strength and elastic modulus, demonstrating the effectiveness of the strategy. This study provides a generalized process monitoring and feedback control method for the 3D printing of continuous fiber-reinforced composites, and offers a potential solution for remote online monitoring and closed-loop adjustment in unmanned or extreme space environments.

1. Introduction

Additive manufacturing, also known as three-dimensional (3D) printing technology, has emerged as a crucial approach in advanced manufacturing because of its various advantages. Among various 3D printing processes, continuous fiber-reinforced polymer composites (CFRPCs) are extensively used in fields such as biomedicine and aerospace owing to their high strength, high modulus, and light weight [1–3]. Unlike 3D printing of pure polymer materials, this process involves the use of continuous fibers combined with a thermoplastic matrix. Both the fiber and matrix materials are simultaneously extruded, followed by rapid cooling and deposition [4–7].

During the 3D printing of CFRPC, the performance of the interface between the fibers and matrix is dependent on the flow rate of the polymer. An improper flow rate of the matrix material can cause issues such as printing path deviation, fiber breakage, fiber pullout, and matrix fracture, thus degrading the performance of the printed components [8,9]. In long-term unmanned or extreme environments, a slight change can result in printing defects. Currently, 3D printing relies predominantly on manual monitoring and adjustment by experienced engineers, which is inconvenient and inefficient.

Therefore, establishing an effective monitoring system for 3D printing is essential to optimize the consistency of part quality. Real-time monitoring of the printing process allows the timely detection and adjustment of printing parameters, thereby promoting the automation of 3D printing processes. In recent years, researchers have monitored the process using different sensors and detected defects caused by inappropriate printing parameters in real time. This allows timely feedback control, representing a critical direction in the current additive manufacturing research domain [10–14]. Remote monitoring based on computer vision, owing to its low cost and noncontact advantages, has been widely employed in various monitoring fields [15,16]. By analyzing images captured on camera, neural network models can be trained to detect printing issues, thus providing possibilities for intelligent 3D printing in unmanned or extreme environments [17,18]. Gu et al. proposed a vision-based fused-deposition modeling 3D printing process detection technology [18,19]. This system efficiently diagnosed the real-time flow rate for polylactic acid (PLA), achieving a prediction accuracy of 98 %.

* Corresponding authors.
E-mail addresses: lingling.wu@xjtu.edu.cn (L. Wu), leoxyt@mail.xjtu.edu.cn (X. Tian).
[1] These authors contributed to this work equally.

https://doi.org/10.1016/j.amf.2025.200196
Received 23 September 2024; Received in revised form 8 December 2024; Accepted 8 December 2024
Available online 22 January 2025
2950-4317/

Since then, research on online monitoring of 3D printing has continued to emerge [20,21]. Researchers have also explored 3D printing process monitoring based on other sensors, such as lasers, temperature, and force [10,22–24].

Despite remarkable achievements in the online monitoring of 3D printing, current research mainly focuses on qualitative prediction. There is a lack of precise quantification and timely feedback control capabilities for real-time printing parameters. Most existing 3D printing equipment employs an open-loop control technology, which makes it difficult to adjust or correct printing parameters during the fabrication process. Furthermore, monitoring technologies for composite materials are relatively scarce, and existing research primarily focuses on pure materials printing. CFRPC 3D printing processes are prone to defects, such as fiber-matrix debonding, which are more difficult to monitor in real time. The datasets of defects of CFRPC 3D printing are also scarce and difficult to identify [25].

Thus, there is an urgent need for the further exploration of online monitoring and closed-loop control technologies for CFRPC 3D printing. To address these issues, this study achieved the quantitative detection and feedback control of the real-time flow rate during a composite 3D printing process. Using PLA as the matrix and carbon fiber as the reinforcing material, this study developed and verified the monitoring and control adjustment of the parameters. By collecting image information near the nozzle with a camera, followed by the introduction of artificial intelligence technology, this study enabled feedback control and dynamic correction under real-time precise defect judgment. This ensured the quality consistency of 3D-printed composites, reducing the reliance on manual intervention and providing optimized strategies for unmanned and extreme environments, such as 3D printing in space [26]. This advancement has promoted the application of 3D-printed CFRPCs in industry.

2. Methods

2.1. Construction of CFRPC 3D printing platform with online monitoring module

To construct an image dataset during the CFRPC 3D printing process, we first constructed a 3D printing platform using an online monitoring module. The camera was installed alongside the nozzle to capture the printed image in real time, as shown in Fig. 1.

PLA was adopted as the matrix material, and carbon fiber was used as the reinforcement material. The online monitoring module (DJI Action 2) was installed on an open-source 3D printer (Original Prusa i3 MK) to capture the image data and provide a basis for the online correction of defects. In this study, we chose the flow rate as the monitoring process parameter to verify our strategy. The flow rate typically refers to the amount of material fed into the nozzle per second by the extruder during the material extrusion 3D printing process. This parameter directly affects the quality and performance of printed parts. An appropriate flow rate ensured uniform material extrusion, thereby maintaining the surface precision and performance of the printed part. Under-extrusion can result in rough surfaces and weak interlayer adhesion, while over-extrusion can compromise the dimensional accuracy and surface quality. The flow rate also affects the interface performance between the fibers and matrix.

To achieve the real-time flow rate through process monitoring, we established remote communication between a 3D printer and Raspberry Pi, an open-source terminal server (OctoPrint) that can connect a computer with a 3D printer with real-time control and dynamic adjustment of printing parameters. A camera was installed alongside the nozzle to capture real-time images during printing. Two neural network models (image segmentation and classification models) were employed to identify online printing defects and parameters. The image segmentation model was utilized to remove the background information and provide more robust input for the image classification model, whereas the image classification model was applied to determine the real-time printing parameters with accurate classes (i.e., flow rates). The printing G-code can be updated based on a closed-loop control strategy to enable the real-time correction of defects caused by abnormal flow rates during printing.

During 3D printing, different line widths require corresponding flow rates to ensure good adhesion between the lines and layers. The calculation of the ideal absolute flow rate E_a for different line widths is shown in Eq. (1).

$$E_a = a \times d \times \frac{c \times h - sf}{\pi r^2} = 0.1247\ \times d, \tag{1}$$

where E_a is ideal absolute flow rate (mm); a is a constant, which usually takes the value of 1 and can be adjusted according to specific printing requirements; r is the filament diameter (mm), with the PLA filament diameter of 1.75 mm; and h is the printing line width. In CFRPC 3D printing, the line width is typically between 1 and 1.2 mm, and should be less than or equal to the nozzle diameter. In this study, a nozzle diameter of 1.3 mm was selected; $c \times h$ is the area of nozzle cross-section (mm^2); sf is the cross-sectional area of the fiber filament, estimated as approximately 0.01 mm^2; $c \times h - sf$ is the cross-sectional area of the melted matrix material (mm^2); and d is the displacement of nozzle (mm).

Eq. (1) can be rewritten as the ideal relative flow rate E shown in Eq. (2).

$$E = a \times \frac{c \times h - sf}{\pi r^2} \approx 0.12, \tag{2}$$

where E is the ideal relative flow rate (dimensionless); the other parameters are consistent with those in Eq. (1).

2.2. Construction of the image dataset for monitoring CFRPC 3D printing

The flow rate should be adjusted based on the specific printing requirements and material characteristics to ensure the quality and performance of the printed composite parts. In this study, we set the line width to 1 mm and calculated the ideal relative flow rate as E = 0.12. This flow rate ensured good interline and interlayer adhesion, avoiding material accumulation or deficiencies. Flow rates higher than 0.12 indicate over-extrusion, whereas lower values indicate under-extrusion.

To quantitatively determine the flow rate during printing, we collected image data of the printing process at eight different flow rates: E = 0.05, 0.08, 0.10, 0.12, 0.15, 0.18, 0.23, and 0.28 (Fig. 2(b)), and constructed an image classification dataset corresponding to these. Through image segmentation, mask prediction, visualization processing, image cropping, and other image operations, as shown in Fig. 2(c), we optimized the image dataset for the neural network model.

During the construction of the image dataset, we first captured videos of the printing process and extracted 100 images per min from the area near the nozzle. Subsequently, all images were resized to 224 × 224 pixels to ensure sufficient feature details while reducing the image size. To enhance the robustness of the image classification model in quantitative recognition and minimize the interference from ambient light, the Mask R-CNN image segmentation model was employed to process raw images. Mask R-CNN generates multiple potential regions of interest by extracting feature maps, and further processes these regions to achieve precise foreground and background segmentation.

By using the Labelme tool, 200 real-time images were annotated, generating JSON format mask files and visualized using OpenCV. The inset of Fig. 2(a) shows the masked areas predicted by the model. Through binarization, we removed the background redundancy and ambient light interference, retaining only the newly printed continuous fiber-reinforced composite material filament area (i.e., the leftmost printed filament area), as illustrated in Figs. 2(a) and (c). The key areas are highlighted in white, while the remainder of the background is black.

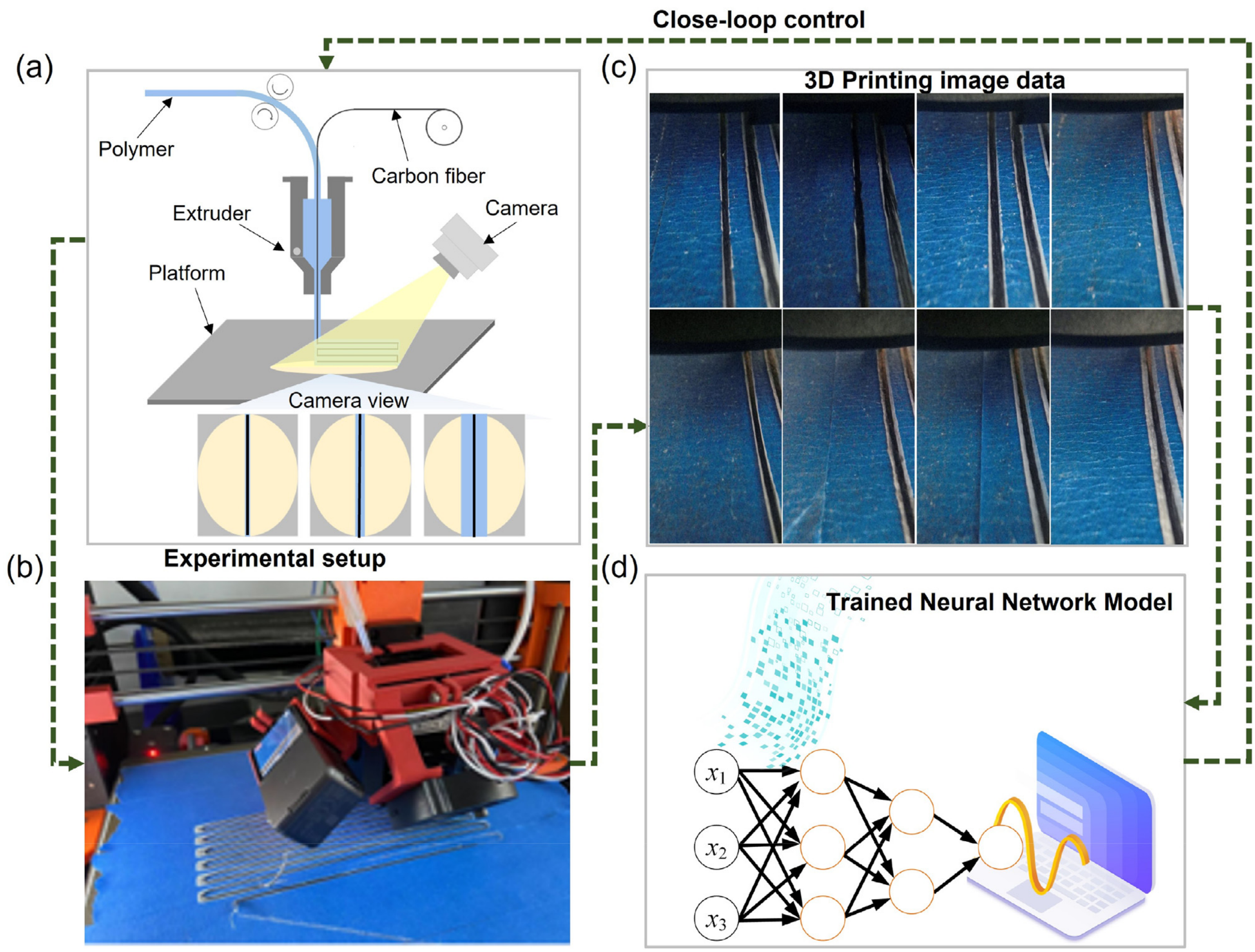

Fig. 1. Global strategy for online monitoring and feedback control of continuous fiber-reinforced polymer composite (CFRPC) 3D printing process: (a) Schematic of the online monitoring setup; (b) Camera installed alongside the nozzle during the CFRPC printing process; (c) 3D printing image captured by the camera with different flow rates; (d) Neural network model trained by the image dataset of CFRPC 3D printing.

The cropped images reduced irrelevant information, making features more prominent and optimizing the training effect of the image classification model. After organizing the raw images and their corresponding visualized masks, we constructed an image-segmentation model dataset for the CFRPC 3D printing process, as shown in Fig. 2(d).

2.3. Neural network model training and verifying

In this study, we chose ResNet50 as the neural network framework to identify the flow rate during the printing process. We trained the ResNet50 neural network model using the dataset to classify the flow rates during the CFRPC 3D printing process. The training results are shown in Figs. 3(a) and (b). The results indicate that after 50 epochs through the dataset, the loss function exhibited a downward trend and the accuracy improved, demonstrating the effectiveness of model training. The model achieved an accuracy of 99.40 % on the training set and an average classification accuracy of 94.70 % on the validation set, indicating high precision in flow rate classification. Fig. 3(c) illustrates the classification accuracy of the model for each flow rate category on the test set. All accuracies exceeded 90 %, confirming the effectiveness of the model.

During printing, the camera-following module captured real-time images near the nozzle and input them into the trained Mask R-CNN model for image segmentation and cropping. The segmented and cropped images were then input into the trained ResNet50 model to quantitatively assess the current flow rate. To avoid errors in flow rate classification caused by a single misidentification, the network recognition results of the first three frames were considered in the quantitative analysis of the flow rate. These results were weighted to assess the real-time flow rate more accurately. Specifically, the classification results of the three frames were multiplied by the weight matrix [0.2, 0.3, 0.5] to obtain the final actual flow rate.

In this study, the ideal relative flow rate was set to 0.12. Based on the detected actual flow rate, the 3D printer code can be updated and corrected according to Eq. (3). Notably, the exact formula for updating the G-code depends on the specific needs of the printing process and material characteristics, ensuring that the flow rate is adjusted dynamically to maintain optimal printing quality and performance.

$$\Delta E = 0.12 - E,\ E' = \Delta E + E, \tag{3}$$

where ΔE is the correction value for the relative flow rate (dimensionless), E is the currently identified relative flow rate value (dimensionless), and E' is the theoretically corrected relative flow rate value (dimensionless).

When the actual flow rate captured in the CFRPC 3D printing process was less than the ideal flow rate of 0.12, the recognition model automatically calculated the corresponding correction value based on the currently identified flow rate. This allowed the G-code to be quantitatively adjusted according to the current flow rate, making the actual extrusion closer to the theoretical ideal flow rate after the breakpoint was identified in the printing process.

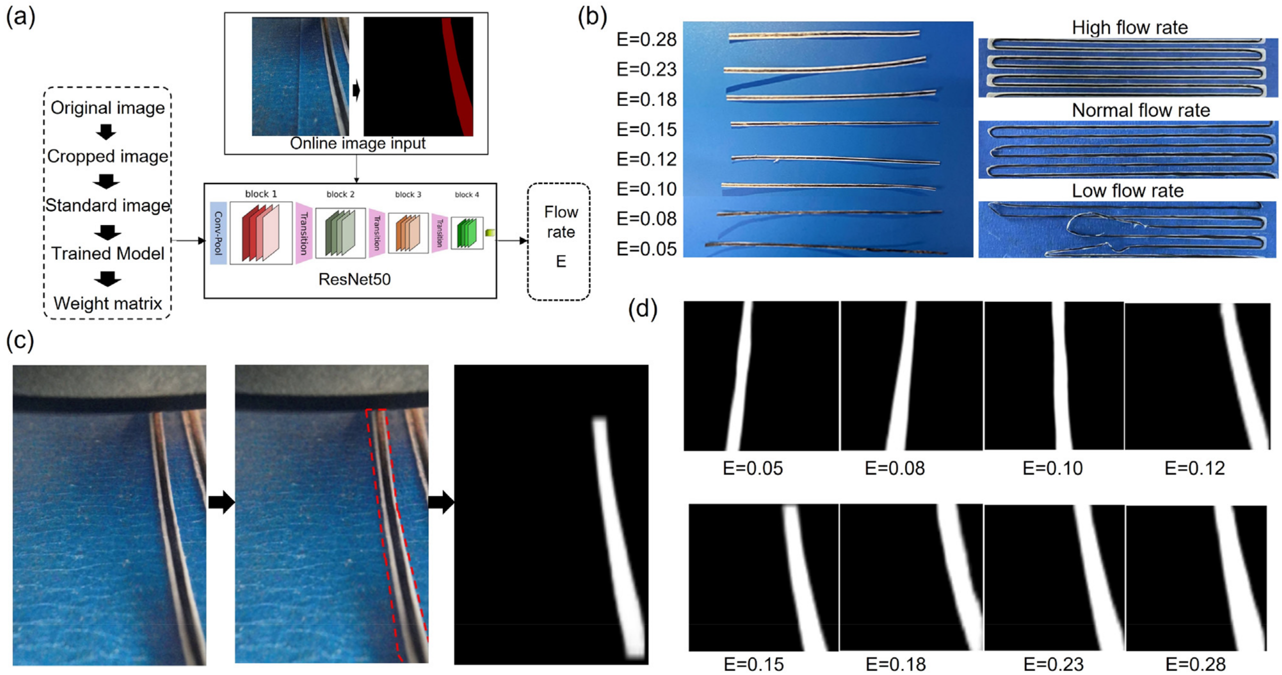

Fig. 2. Construction of dataset for neural network model: (a) Schematic of the neural network model for continuous fiber-reinforced polymer composite (CFRPC) 3D printing process monitoring; (b) CFRPC 3D printing quality under different flow rates; (c) Image treatment process to build the dataset; (d) Construction of the composite material 3D printing dataset.

3. Experimental Results

To evaluate the performance of the precise identification and quantitative feedback control technology for printing defects and parameters during the printing process, we designed single- and multilayer printing test schemes for CFRPC 3D printing along with the corresponding performance evaluation indicators. In the CFRPC process, under-extrusion defects are more likely to result in print failure, whereas over-extrusion predominantly affects the line width accuracy. Therefore, under-extrusion, rather than over-extrusion, was identified as the primary factor contributing to print failure. Consequently, the experimental validation focused on examining the flow rate variations from under-extrusion to over-extrusion.

3.1. Single-layer printing test

In the experiment, the initial flow rate was set to a nonideal state ($E = 0.05$). Through online quantitative identification and adaptive correction, the flow rate gradually approached the ideal value. The effectiveness of this strategy was evaluated by comparing the corrected regions. A camera-following 3D printing platform was used for real-time monitoring, and a single-layer Z-shaped path was selected as the printing path. The horizontal width of the single-layer component was 150 mm, the printing line width was set to 1 mm, and the printing speed was 20 mm/s. According to Eqs. (1) and (2), the corresponding ideal flow rate for this printing parameter setting was approximately 0.12.

Optical microscopy (Zeiss Axio Scope A1) and laser scanning surface morphology observations were used for the qualitative and quantitative analyses of the performance differences of the single-layer prints before and after correction. As shown in the optical microscopy images in Fig. 3(d), the initial printing of the single-layer construct exhibited insufficient extrusion of the white matrix material, resulting in large gaps between the filaments and poor fiber-matrix bonding, indicating an under-extrusion state. After adaptive quantitative adjustment of the flow rate, the extrusion of the matrix material significantly increased, the gaps between filaments noticeably decreased, and the fiber–matrix interface effectively improved, thereby validating the effectiveness of this method for adjusting and correcting the flow rate during the printing process.

To further evaluate the surface morphology of the continuous fiber-reinforced composite single-layer prints before and after the adaptive correction of the flow rate, three-coordinate laser scanning technology was used to scan the single-layer prints obtained from the experiment, acquiring approximately 200 000 surface morphology observation points. After filtering the scanned data, the three- and two-dimensional visualization effects are shown in Figs. 3(e) and (f), respectively. Before correction, significant fluctuations were observed in the vertical Z-direction; after correction, the vertical fluctuations of the printed parts were smoother. Compared with the under-extruded areas before correction, the corrected printed parts exhibited a more even surface, demonstrating better surface quality.

3.2. Multilayer printing test

To evaluate the effect of process monitoring and feedback control technology on the mechanical performance of 3D printed CFRPC parts, we conducted microscopic observations and tensile performance testing on the multilayer printed samples, as shown in Fig. 4. Owing to the size limitations of the printer's build plate, the length of the multilayer printed parts was set to 12 cm, with a printing scan gap of 1 mm and printing speed of 20 mm/s. The initial flow rate was set to an under-extrusion state ($E = 0.05$). Two sets of experiments, uncorrected and corrected, were conducted with a 1 mm line width.

Similar to the single-layer experiment, the experiment also started from a nonideal flow state of 0.05, with online identification and adaptive correction, bringing the flow rate closer to the ideal value. The experiments were divided into an uncorrected control group and a corrected group using correction technology, both of which employed a long strip-shaped multilayer printing structure. The mechanical performance testing of the printed parts was conducted using an MTS-CMT4304 static testing machine to evaluate the tensile strength and elastic modulus.

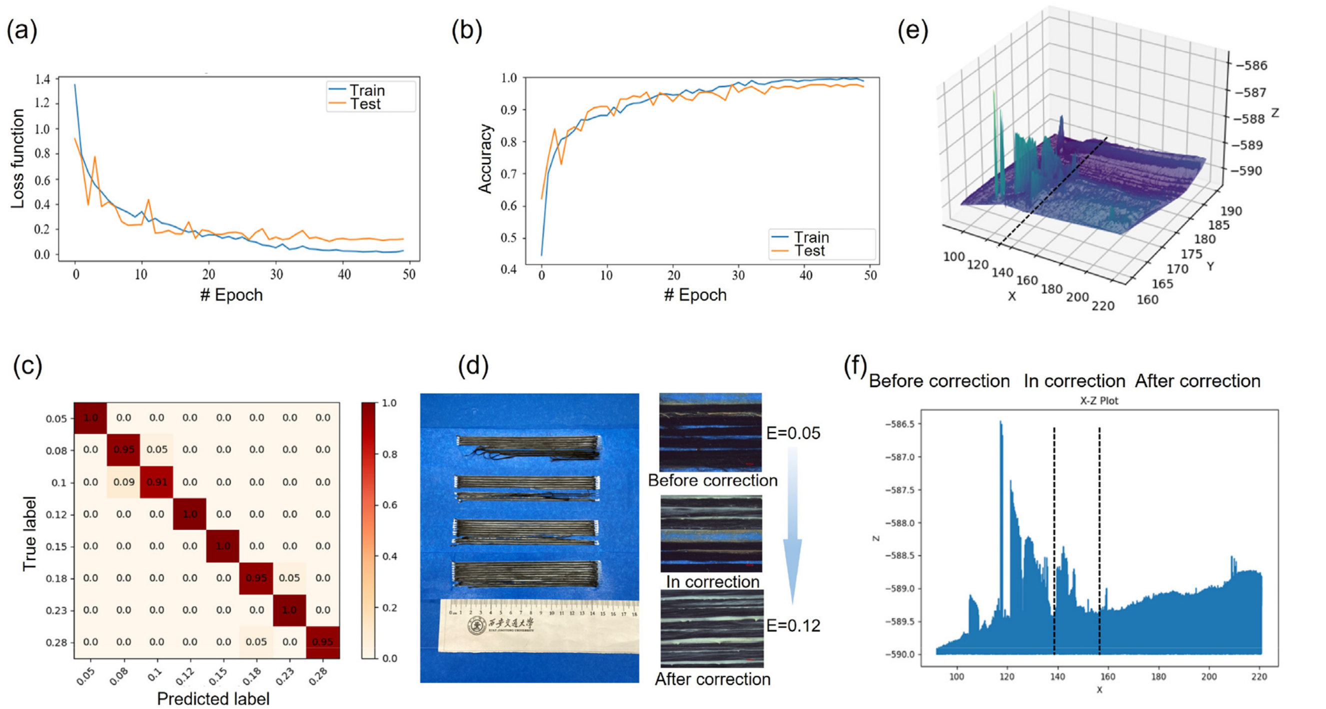

Fig. 3. Training the ResNet50 neural network model using the continuous fiber-reinforced polymer composite 3D-printing dataset and experimental verification of single-layer test: (a) Evolution of the loss function during the training process; (b) Evolution of the prediction accuracy during the training process; (c) Confusion matrices of the final network after the training on our test dataset for flow rate; (d) Correction of prints started with incorrect flow rate parameter; (e) Laser scanning surface morphology observation; (f) Cross-section data from laser scanning surface morphology observation.

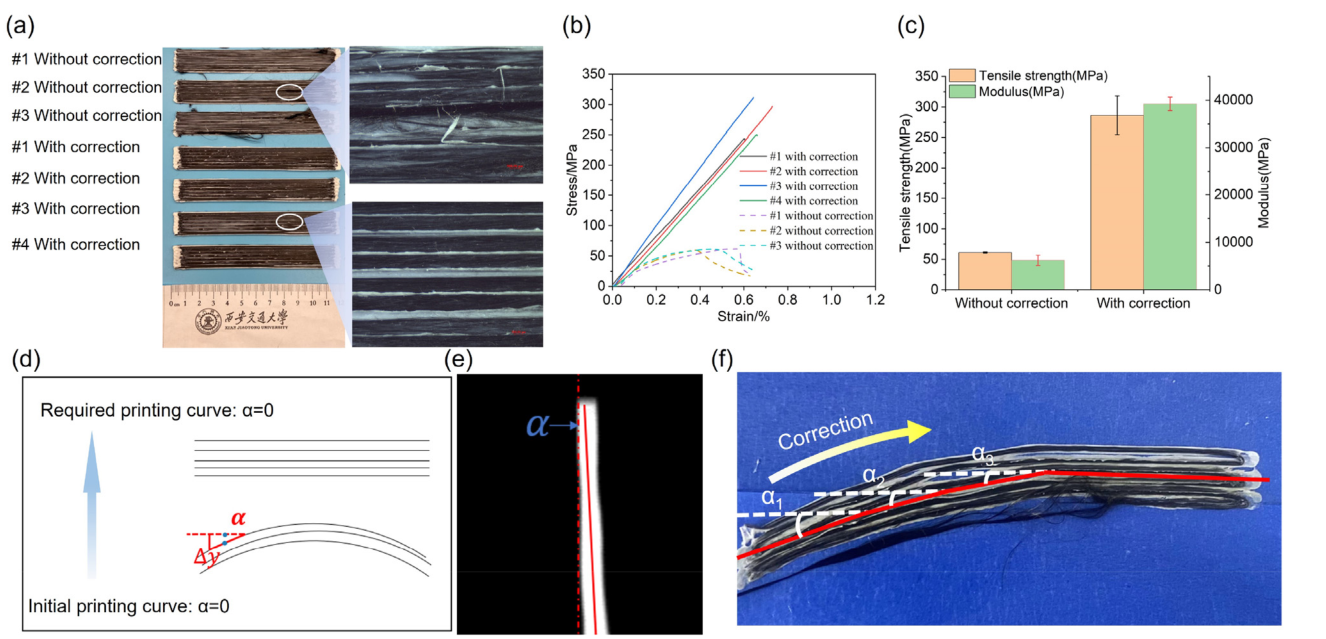

Fig. 4. Measurement results of multilayer printed parts in the continuous fiber-reinforced polymer composite 3D-printing process, with and without online monitoring and correction, along with the print path correction results: (a) Photos of the sample without and with correction; (b) Stress-strain curves of the sample without and with correction from tensile testing; (c) Tensile strength (MPa) and modulus (MPa) of the stretched and unstretched sample; (d) Diagram showing the deviation angle α, defined as the angle between the actual position of the printed filament and target direction; (e) Printed path processed using OpenCV, with analysis of the deviation angle α between the target and actual paths; (e) Photo showing the gradual correction of the deviation angle α during the printing process.

The corrected parts utilized a camera-following module to capture real-time images, identifying the flow rate through the neural network model and making adaptive adjustments. The uncorrected group continued printing with the initial flow rate without adjustments. Comparison of the uncorrected and corrected prints showed that the uncorrected samples exhibited fiber-matrix adhesion issues and poor surface quality.

Tensile performance evaluations were conducted on the corrected and uncorrected multilayer CFRPC-printed parts. The experimental results indicate that the uncorrected samples had poor fiber-matrix interfaces, leading to fiber breakage and reduced mechanical performance. The corrected parts performed better in tensile tests, showing no instances of filament breakage.

The tests included four groups of printed parts: corrected and uncorrected samples with a 1 mm line width. The results showed significant improvements in the mechanical performance of the corrected samples on the stress-strain curve, as shown in Fig. 4(b). The tensile strength increased from 60.98 ± 1.02 MPa in the uncorrected samples to 286.28 ± 31.88 MPa in the corrected samples, an approximately four-fold improvement. The elastic modulus increased from 6207.29 ± 1084.6 MPa in the uncorrected samples to 39,240.18 ± 1407.5 MPa in the corrected samples, indicating that the corrected samples exhibited less deformation under the same load, as shown in Fig. 4(c). The mechanical performance of the uncorrected samples showed large fluctuations and poor quality consistency, where the corrected samples demonstrated better performance stability and consistency. These results validate the effectiveness of the adaptive adjustment strategy in improving the performance and quality consistency of continuous fiber-reinforced 3D printed parts.

3.3. Printing path correction verification

This study also determined the filament deviation angle during printing and designed a real-time detection and feedback control strategy for the printing path. The camera-following module captured real-time images near the nozzle. The deviation angle α is defined as the angle between the actual position of the printed filament and the target direction, as shown in Fig. 4(d).

The study selected a horizontal line as the target contour, and conducted deviation angle monitoring and feedback control experiments. Building on the single-layer Z-shaped path experiment (width 150 mm, line gap 1.2 mm, and nozzle speed 20 mm/s), an initial deviation angle $\alpha \neq 0$, $\alpha = 0$ was set. Through identification, monitoring, and closed-loop control, the target contour was approached. The camera-following module captured real-time images, which were processed by an image segmentation model and OpenCV tools to identify the deviation angle, as shown in Fig. 4(e). A strategy was developed for updating and adjusting the G-code based on different target shapes to bring the detected shape deviations of the printed part closer to the ideal contour. This strategy is illustrated in Eq. (4).

$$x' = x + \Delta x,\ y' = y + \Delta y \tag{4}$$

where x' is the corrected theoretical x-coordinate value (mm), x is the original x-coordinate value in the G-code (mm), Δx is the x-coordinate correction value (mm), y' is the corrected theoretical y-coordinate value (mm), y is the original y-coordinate value in the G-code (mm), and Δy is the y-coordinate correction value (mm).

When the target contour was a horizontal line, only the vertical y-direction was corrected. At a deviation angle of $\alpha > 0$, $\Delta y > 0$ resulted in an upward translation of the updated printing path in the y-direction. Conversely, at a deviation angle of $\alpha < 0$, $\Delta y < 0$ resulted in a downward translation of the updated printing path in the y-direction. This correction brings the printed part closer to the horizontal target contour, as expressed in Eq. (5).

$$\Delta x = 0, \Delta y = \frac{l \sin \alpha}{2}, \tag{5}$$

where $\Delta x, \Delta y$: x, y are the correction values for the x and y coordinates (mm), respectively, l is a constant representing the step size set for adjusting the x and y coordinates (mm), and α is the currently identified deviation angle of the printed filament (°).

The experiment showed that after updating the G-code, as shown in Fig. 4(f), the printing path was closer to the ideal contour, while simultaneously performing quantitative online identification and adaptive adjustment of the flow rate. The results indicated that the feedback-adjusted prints were closer to the horizontal contour, with significantly improved fiber-matrix adhesion, validating the applicability of the adaptive printing parameters and path adjustment strategy, as shown in Fig. 4(f). Building on this work, future efforts will be directed toward optimizing the printing path at turning points, with the aim of reducing defects at these locations in the CFRPC printing process and enhancing the dimensional accuracy of the formed structures at the turning points.

4. Conclusions

This study proposed an online monitoring and closed-loop control technology for CFRPC 3D printing processes based on a machine learning method. The aim is to address the challenges of real-time defect detection and feedback adjustment during printing. An online monitoring platform suitable for the CFRPC 3D printing process was constructed, and a camera-following monitoring module with a closed-loop control module was developed on the Prusa MK i3 printer, enabling the precise detection and remote control of the relative flow rate. A neural network model based on computer vision and machine learning was developed for the online monitoring and prediction of printing parameters during the 3D printing of CFRPCs. The model achieved a prediction accuracy of 94.70 %. It also enhanced the robustness of monitoring in variable environments. The effectiveness of the online monitoring and correction strategy for printing parameters were experimentally verified. The corrected components exhibited superior surface precision and a three to six times enhancement of the mechanical properties of printed components. In addition, we determined the filament deviation angle during printing and designed a real-time qualitative detection and feedback control strategy for the printing path.

This study validated the effectiveness of online monitoring and real-time adjustment technology in the CFRPC 3D printing process. Future research should focus on multiparameter monitoring. While the current model primarily monitors the flow rate, future efforts can include online monitoring and feedback control of other printing parameters, such as printing speed, nozzle temperature, and nozzle height, to achieve a more comprehensive process optimization. In addition, existing strategies only process surface images and cannot detect internal defects. Future enhancements could involve the combination of thermometers, force sensors, or ultrasonic sensors to acquire more comprehensive printing data, thereby improving the accuracy of monitoring and adjustments, which possess significant potential in unmanned or long-duration operational environments.

Declaration of competing interest

The authors declare that they have no known competing financial interests or personal relationships that could have influenced the work reported in this paper.

CRediT authorship contribution statement

Xinyun Chi: Writing – original draft, Visualization, Methodology, Investigation. **Jiacheng Xue:** Methodology, Investigation, Writing – original draft. **Lei Jia:** Writing – review & editing, Investigation. **Jiaqi Yao:** Methodology, Writing – review & editing. **Huihui Miao:** Writing – review & editing, Methodology. **Lingling Wu:** Writing – review & editing, Funding acquisition, Conceptualization. **Tengfei Liu:** Writing – review & editing, Methodology, Investigation. **Xiaoyong Tian:** Writing – review & editing, Resources, Funding acquisition. **Dichen Li:** Writing – review & editing, Resources, Funding acquisition.

Acknowledgements

This work was supported by National Key Research and Development Program of China (Grant No. 2023YFB4604100), National Key Research and Development Program of China (Grant No. 2022YFB3806104), Key Research and Development Program in Shaanxi Province (Grant No. 2021LLRH-08-17), Young Elite Scientists Sponsorship Program by CAST (No. 2023QNRC001), K C Wong Education Foundation of China, Youth Innovation Team of Shaanxi Universities of China, and Key Research and Development Program of Shaanxi Province (Grant 2021LLRH-08-3.1).

Supplementary materials

Supplementary material associated with this article can be found, in the online version, at doi:10.1016/j.amf.2025.200196.

References

[1] Kabir SMF, Mathur K, Seyam AFM. A critical review on 3D printed continuous fiber-reinforced composites: History, mechanism. Materials and properties. Compos Struct 2020;232:111476.
[2] Hu Y, Ladani RB, Brandt M, et al. Carbon fibre damage during 3D printing of polymer matrix laminates using the FDM process. Mater Des 2021;205:109679.
[3] Wei H, Tang L, Qin H, et al. Optimizing FDM 3D printing parameters for improved tensile strength using the Takagi–Sugeno fuzzy neural network. Mater Today Commun 2024;38:108268.
[4] Tian X, Todoroki A, Liu T, et al. 3D printing of continuous fiber reinforced polymer composites: Development, application, and prospective. Chinese J Mech Eng:Additive Manufacturing Frontiers 2022;1(1):100016.
[5] Tian X, Wu L, Gu D, et al. Roadmap for additive manufacturing: Toward intellectualization and industrialization. Chinese J Mech Eng:Additive Manufacturing Frontiers 2022;1(1):100014.
[6] Tian X, Liu T, Yang C, et al. Interface and performance of 3D printed continuous carbon fiber reinforced PLA composites. Composites Part A: Applied Science and Manufacturing 2016;88:198–205.
[7] Liu T, Tian X, Zhang M, et al. Interfacial performance and fracture patterns of 3D printed continuous carbon fiber with sizing reinforced PA6 composites. Composites Part A: Applied Science and Manufacturing 2018;114:368–76.
[8] Parandoush P, Tucker L, Zhou C, et al. Laser assisted additive manufacturing of continuous fiber reinforced thermoplastic composites. Mater Des 2017;131:186–95.
[9] Zhang H, Chen J, Yang D. Fibre misalignment and breakage in 3D printing of continuous carbon fibre reinforced thermoplastic composites. Addit Manuf 2021;38:01775.
[10] AbouelNour Y, Gupta N. Assisted defect detection by in-process monitoring of additive manufacturing using optical imaging and infrared thermography. Addit Manuf 2023;67:103483.
[11] Holzmond O, Li X. In situ real time defect detection of 3D printed parts. Addit Manuf 2017;17:135–42.
[12] Bisheh MN, Chang SI, Lei S. A layer-by-layer quality monitoring framework for 3D printing. Comput Ind Eng 2021;157:107314.
[13] Ogunsanya M, Isichei J, Parupelli SK, et al. In-situ droplet monitoring of inkjet 3D printing process using image analysis and machine learning models. Procedia Manuf 2021;53:427–34.
[14] Westphal E, Seitz H. Machine learning for the intelligent analysis of 3D printing conditions using environmental sensor data to support quality assurance. Addit Manuf 2022;50:102535.
[15] Torralba A, Russell BC, Yuen J. Labelme: Online image annotation and applications. Proc IEEE 2010;98(8):1467–84.
[16] He K, Zhang X, Ren S, et al. Deep residual learning for image recognition. In: Proceedings of 2016 IEEE Conference on Computer Vision and Pattern Recognition, 27-30 June, Las Vegas, NV, USA; 2016.
[17] Rill-García R, Dokladalova E, Dokládal P, et al. Inline monitoring of 3D concrete printing using computer vision. Addit Manuf 2022;60:103175.
[18] Jin Z, Zhang Z, Gu GX. Autonomous in-situ correction of fused deposition modeling printers using computer vision and deep learning. Manuf Lett 2019;22:11–15.
[19] Jin Z, Zhang Z, Ott J, et al. Precise localization and semantic segmentation detection of printing conditions in fused filament fabrication technologies using machine learning. Addit Manuf 2021;37:101696.
[20] Wright WJ, Darville J, Celik N, et al. In-situ optimization of thermoset composite additive manufacturing via deep learning and computer vision. Addit Manuf 2022;58:102985.
[21] Brion DAJ, Pattinson SW. Generalisable 3D printing error detection and correction via multi-head neural networks. Nat Commun 2022;13(1):4654.
[22] Vallabh CKP, Zhang Y, Zhao X. In-situ ultrasonic monitoring for vat photopolymerization. Addit Manuf 2022;55:102801.
[23] Lu L, Yuan S, Yao X, et al. In-situ process evaluation for continuous fiber composite additive manufacturing using multisensing and correlation analysis. Addit Manuf 2023;74:103721.
[24] Petrich J, Snow Z, Corbin D, et al. Multi-modal sensor fusion with machine learning for data-driven process monitoring for additive manufacturing. Addit Manuf 2021;48:102364.
[25] Lu L, Hou J, Yuan S, et al. Deep learning-assisted real-time defect detection and closed-loop adjustment for additive manufacturing of continuous fiber-reinforced polymer composites. Robot Comput Integr Manuf 2023;79:102431.
[26] Liu T, Zhang M, Kang Y, et al. Material extrusion 3D printing of polyether ether ketone in vacuum environment: Heat dissipation mechanism and performance. Addit Manuf 2023;62:103390.